

Effects of Earthquake Magnitude, Distance, and Site Conditions on Spectral and Pseudospectral Velocity Relationship

Haizhong Zhang¹ and Yan-Gang Zhao^{*1}

ABSTRACT

The spectral velocity (SV) is necessary information in the seismic design of structures with supplemental velocity-dependent dampers, and it is conventionally approximated by the pseudospectral velocity (PSV), which is available in seismic codes. Because of the significant approximation error, it is important to clarify the relationship between the two spectra to establish a suitable formulation to relate SV to PSV. Recent studies have point out that this relationship is influenced not only by the oscillator period and damping ratio but also by earthquake characteristics (Papagiannopoulos *et al.*, 2013; Samdaria and Gupta, 2018). To clarify the seismological effects, in this study, an approach to relate SV to PSV based on the random vibration theory is proposed, and it is verified by comparing its results with those of traditional time-series analysis. The effects of earthquake magnitude and distance as well as site conditions on the relationship between the two spectra are explored based on the proposed approach as well as statistical analysis of recorded seismic motions. It is found that the SV approaches the PSV with increasing magnitudes at long oscillator periods but performs oppositely at short oscillator periods. The demarcation range beyond which the opposite trend is observed varies from (0.07–0.24) to (0.12–0.87) s using the proposed approach and considering the regions of central and eastern North America. The range varies from (0.1–0.15) to (0.3–0.7) s based on the results obtained by the statistical analysis of seismic records in Japan. The observed phenomena were theoretically explained, and the seismological effects were found to be governed by the ground-motion frequency content.

KEY POINTS

- This study aims to clarify the seismological effects on the spectral and pseudospectral velocity relationship.
- Spectral velocity approaches pseudospectral velocity with increasing magnitudes at long oscillator periods.
- The conclusions are useful for constructing reasonable spectral velocity for seismic design.

INTRODUCTION

The response spectrum has been the most popular tool for characterizing seismic hazards for structural designs because it enables the convenient assessment of maximum response. A variety of response spectra can be defined depending on the plotted maximum response quantity, including spectral displacement, spectral velocity (SV), spectral acceleration, pseudospectral velocity (PSV), and pseudospectral acceleration (PSA). Of these, only the PSA is typically given out in seismic codes to characterize seismic hazards (Eurocode 8, 2004; ASCE/SEI7-10, 2011).

Nevertheless, for the seismic design of structures equipped with supplemental velocity-dependent dampers, the SV is necessary to calculate the peak relative velocity values across the ends of dampers and determine their design forces (Federal Emergency Dissipation Agency [FEMA-450], 2003). Because of the absence of information on SV in seismic codes, the SV is conventionally approximated by the PSV converted from the PSA (FEMA-450, 2003). However, Sadek *et al.* (2000) pointed out that this approximation is only valid over the intermediate-period range. Over shorter oscillator periods, the SV ordinate is smaller than that of the PSV, whereas over longer oscillator periods, the SV ordinate is larger and increases with the increase in the oscillator period and damping ratio. Sadek *et al.* (2000) developed a simple formulation to relate SV to PSV based on the statistical analyses of 72 accelerograms from

1. Department of Architecture, Kanagawa University, Yokohama, Japan

*Corresponding author: zhaog@kanagawa-u.ac.jp

Cite this article as Zhang, H., and Y.-G. Zhao (2021). Effects of Earthquake Magnitude, Distance, and Site Conditions on Spectral and Pseudospectral Velocity Relationship, *Bull. Seismol. Soc. Am.* **111**, 3160–3174, doi: [10.1785/012021015](https://doi.org/10.1785/012021015)

© Seismological Society of America

36 stations in the western United States. Subsequently, [Song et al. \(2007\)](#) theoretically discussed the relationship between the two spectra and developed an analytical approach to predict SV from a 5% damped PSV. [Gupta \(2009\)](#) derived a simpler formulation to relate SV to PSV, and it is suitable for short oscillator periods. [Papagiannopoulos et al. \(2013\)](#) developed formulations to relate the two spectra based on the statistical analysis of 866 accelerograms from various earthquakes recorded worldwide. Moreover, using 172 ground motions selected from all over the world, [Desai and Tande \(2017\)](#) proposed an empirical formulation for longer oscillator periods (>0.86 s) for a 5% damping ratio. [Samdaria and Gupta \(2018\)](#) further analyzed the relationship between SV and PSV and proposed a formulation for long oscillator periods of up to 15 s by statistically analyzing 205 ground motions from 36 earthquake events in the western United States. [Desai and Tande \(2018\)](#) developed a bifunctional model to estimate SV from PSV based on the statistical analysis of 108 ground motions. [Pal and Gupta \(2021\)](#) further extended the formulas of [Gupta \(2009\)](#) to a wider range of periods with the help of a suite of 464 ground motions.

All of these studies agree that the relationship between SV and PSV is influenced by the oscillator period and damping ratio. Thus, most of them have incorporated the two parameters into their formulations for determining SV from PSV. [Papagiannopoulos et al. \(2013\)](#) and [Samdaria and Gupta \(2018\)](#) found from statistical and theoretical analyses that this relationship is also influenced by ground-motion characteristics, which are essentially determined by the earthquake source and path as well as site conditions. Although several empirical formulations for determining SV from PSV that partly consider seismological effects have been developed ([Desai and Tande, 2017](#); [Samdaria and Gupta, 2018](#)), how the seismological parameters affect the relationship between the two spectra has never been systematically discussed and clearly understood, which is basic and critical knowledge for constructing a reasonable formulation to relate SV to PSV.

This study aims at clarifying the seismological effects on the SV–PSV relationship. The rest of the article is organized as follows. First, an approach for estimating the SV to PSV ratio is proposed based on the random vibration theory (RVT) and is verified by comparing its results with those of traditional time-series analyses. Then, the effects of earthquake magnitude and distance as well as site conditions on the SV–PSV relationship are systematically explored and explained based on the proposed approach. Subsequently, the seismological effects are further explored based on the statistical analysis of real seismic records. Finally, the conclusions are presented.

SV/PSV BASED ON RVT

Equation for SV/PSV

To explore the seismological effects on the SV–PSV relationship, an equation for SV/PSV is derived based on the RVT in

this section. The RVT states that the peak value of a signal is equal to the product of its root mean square (rms) value and an estimated peak factor. Based on this principle, [Boore \(2003\)](#) derived an equation for the PSV of earthquake ground motion, and it is expressed as follows:

$$\text{PSV}(\bar{\omega}, \xi) = pf_{p\xi} \sqrt{\frac{1}{Dp_{\text{rms}}\pi} \int_0^\infty |\text{YR}(\omega, \bar{\omega}, \xi)|^2 d\omega}, \quad (1)$$

in which the square root part of equation (1) and $pf_{p\xi}$ denote the rms velocity and peak factor of the single-degree-of-freedom (SDOF) oscillator response, respectively; $\bar{\omega}$ and ξ are the circular frequency and damping ratio of the SDOF oscillator, respectively; and Dp_{rms} is the oscillator-response duration. Moreover, $\text{YR}(\omega, \bar{\omega}, \xi)$ is the Fourier amplitude spectrum (FAS) of the oscillator response, which is equal to the product of the ground-acceleration FAS, $Y(\omega)$, with the absolute value of the oscillator transfer function for the PSV, $|\text{Hpv}(\omega, \bar{\omega}, \xi)|$,

$$\text{YR}(\omega, \bar{\omega}, \xi) = Y(\omega) |\text{Hpv}(\omega, \bar{\omega}, \xi)|, \quad (2)$$

$$|\text{Hpv}(\omega, \bar{\omega}, \xi)| = \frac{\bar{\omega}}{\sqrt{(2\xi\omega\bar{\omega})^2 + (\omega^2 - \bar{\omega}^2)^2}}, \quad (3)$$

in which ω is the circular frequency of FAS. It is important to keep in mind the difference between the oscillator circular frequency $\bar{\omega}$ and the circular frequency of FAS ω .

Similarly, the SV can be obtained based on the RVT by replacing the oscillator-response peak factor and duration as well as the oscillator transfer function for PSV in equation (1) with those for SV. The oscillator transfer function for SV $\text{Hv}(\omega, \bar{\omega}, \xi)$ is expressed as follows:

$$|\text{Hv}(\omega, \bar{\omega}, \xi)| = \frac{\omega}{\sqrt{(2\xi\omega\bar{\omega})^2 + (\omega^2 - \bar{\omega}^2)^2}}. \quad (4)$$

Then, SV/PSV is obtained as the ratio of SV to PSV, which is expressed as follows:

$$\frac{\text{SV}(\bar{\omega}, \xi)}{\text{PSV}(\bar{\omega}, \xi)} = \sqrt{\frac{\int_0^\infty |Y(\omega)\text{Hv}(\omega, \bar{\omega}, \xi)|^2 d\omega / D_{\text{rms}}}{\int_0^\infty |Y(\omega)\text{Hpv}(\omega, \bar{\omega}, \xi)|^2 d\omega / Dp_{\text{rms}}}} \times \frac{pf_\xi}{pf_{p\xi}}, \quad (5)$$

in which pf_ξ and D_{rms} are the oscillator-response peak factor and duration for SV, respectively. Equation (5) is the product of two terms. The first term represents the ratio of the oscillator-response rms velocities of SV to PSV (hereafter referred to as rms ratio, R_{rms}). The second term represents the ratio of the oscillator-response peak factors of SV to PSV (hereafter referred to as peak factor ratio, R_{pf}).

When equation (5) is applied to determine SV/PSV, the oscillator-response durations for SV and PSV need to be determined. Because the oscillator-response duration for SV D_{rms} has not been discussed yet, D_{rms} is assumed to be the same as that for PSV Dp_{rms} , which can be estimated using the equation of Boore and Thompson (2015). The oscillator-response peak factors also need to be determined for the calculation of SV/PSV. Many peak factor models have been developed for RVT analyses (Cartwright and Longuet-Higgins, 1956; Davenport, 1964; Vanmarcke, 1975). Although the Cartwright and Longuet-Higgins (1956) model has been commonly applied in engineering seismology and site-response analyses (Rathje and Ozbey, 2006), the Vanmarcke (1975) model can give better estimations of the peak factor (Wang and Rathje, 2016). The cumulative distribution function of the peak factor, pf , provided by Vanmarcke (1975) is expressed as follows:

$$P(pf < r) = [1 - e^{(-r^2/2)}] \times \exp\left[-2f_z \exp(-r^2/2) D \frac{(1 - e^{-\delta^{1.2} r \sqrt{\pi/2}})}{(1 - e^{-r^2/2})}\right], \quad (6)$$

in which D is the signal duration and δ is the bandwidth factor of FAS, which is defined as a function of the spectral moments of FAS as follows:

$$\delta = \sqrt{1 - \frac{m_1^2}{m_0 m_2}}, \quad (7)$$

in which m_0 , m_1 , and m_2 are the zeroth-, first-, and second-order spectral moments of FAS, respectively, and the i th-order spectral moment is defined as follows:

$$m_n = \frac{1}{\pi} \int_0^\infty \omega^n |Y(\omega)|^2 d\omega, \quad (8)$$

f_z in equation (6) is the rate of zero crossing, and it is defined as follows:

$$f_z = \frac{1}{2\pi} \sqrt{\frac{m_2}{m_0}}. \quad (9)$$

In RVT analyses, the expected value of pf is typically used. According to equation (6), the expected value of pf is obtained by $\int_0^\infty [1 - P(pf < r)] dr$.

When equation (5) is applied to determine SV/PSV, the ground-acceleration FAS also needs to be determined. Various methods are available for describing ground-acceleration FAS. The simplest approach involves the use of seismology theory to estimate FAS from a point source in terms of various sources, paths, and site parameters. This article utilized the FAS model given by Boore (2003). The acceleration FAS at

a rock site, $Y(\omega)$, is expressed as a function of the source, path, and site characteristics. The details of this model can be found in Boore (2003) and Zhang and Zhao (2020). The model requires information on various seismological parameters, for example, stress drop $\Delta\sigma$, site diminution k , mass density of the crust ρ , shear-wave velocity of the crust β , geometrical attenuation $Z(R)$, anelastic attenuation $Q(f)$, and crustal amplification $A(f)$. The seismological parameters for the regions of central and eastern North America were used in this study because of a recent work that updated the seismological parameters for these regions (Boore and Thompson, 2015), as summarized in table 1 of Wang and Rathje (2016). The values of these parameters may differ for other regions in the world, leading to various values of SV and PSV and resulting in different SV/PSV values. Nevertheless, the trends of SV/PSV with the variations in the main seismological parameters considered in this study are basically consistent even for different regions, as supported by the following discussions. Because the model incorporates the properties of the earthquake source and path as well as site conditions, it allows the systematic exploration of the seismological effects. A flowchart of the proposed approach is presented in Figure 1.

Comparison with time-series analysis

To investigate the accuracy of the proposed approach, its predicted results are compared with those calculated using traditional time-series analyses. Wide ranges of the oscillator period T_0 (0.03–10 s), damping ratio ξ (5%–50%), and main seismological parameters, including the moment magnitude M (4.0–8.0) and site-to-source distance R (20–200.01 km), are considered in the calculations. Determining the site-to-source distance value also considers the simplicity of calculation. The equation for the oscillator-response duration Dp_{rms} by Boore and Thompson (2015) requires many coefficients, which correspond to discrete distances (e.g., 200.01 km). To avoid interpolation, the distances for which these coefficients can be directly obtained are used. Then, 36 FASs are obtained based on the model of Boore (2003). The corner frequency, representing the frequency below which the FAS decays, varies from 0.06 to 6 Hz. The time series used for the verification are generated from the FAS using the Stochastic-Method SIMulation (Boore, 2005) program. For each FAS, a suite of 100 time-series accelerations is generated via stochastic simulation (Boore, 1983); the average FAS of the generated time series matches the given FAS. Then, the values of SV/PSV for all of the generated time series are calculated using the direct integration method of Nigam and Jennings (1969). For each FAS, the 100 corresponding results of SV/PSV for a given damping level are averaged and compared with those obtained using the proposed approach. Some of these representative comparisons are shown in Figures 2–4.

It is evident from these figures that, although the results of the proposed approach do not agree very well with those of the

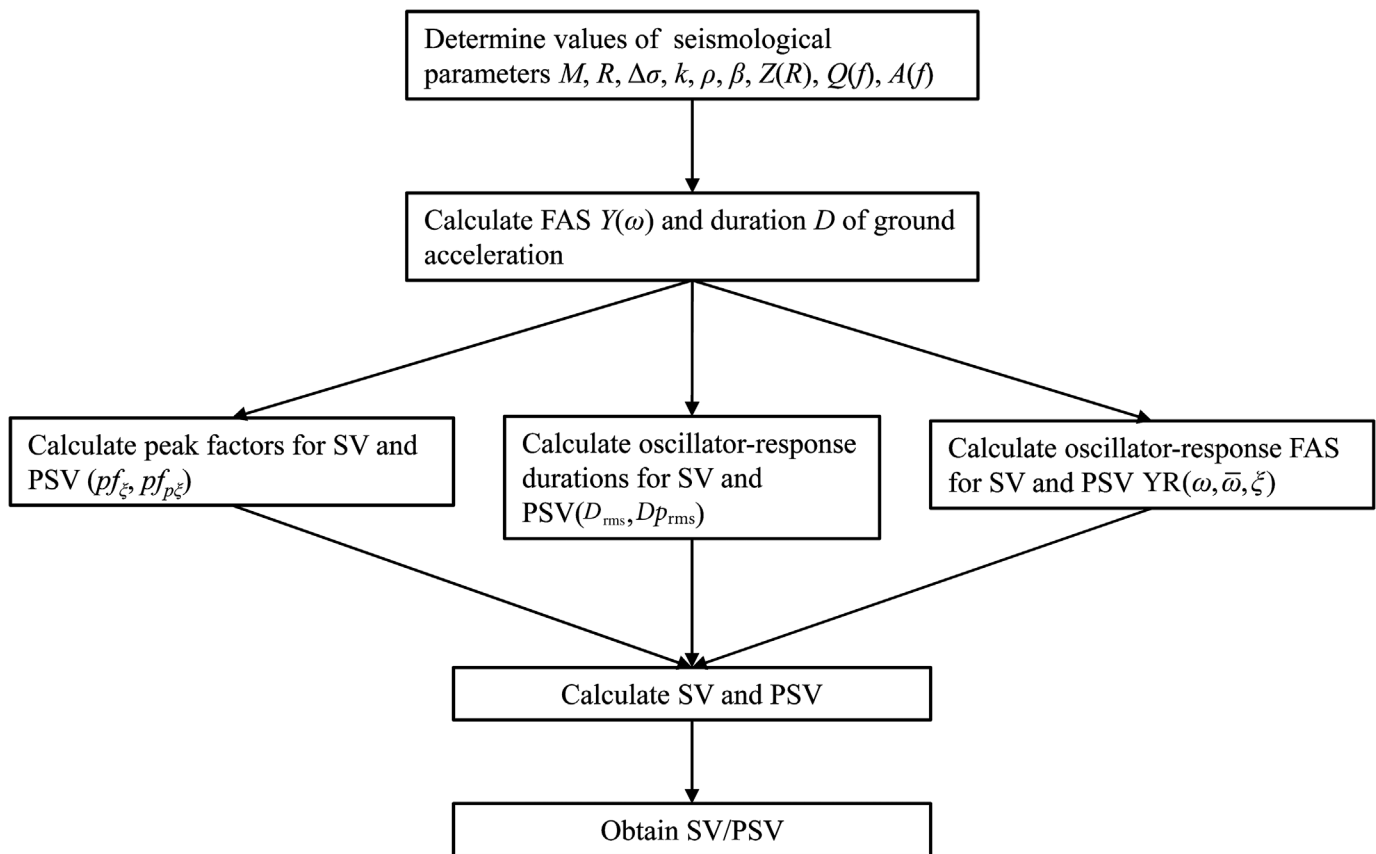


Figure 1. Flowchart of the proposed approach for spectral velocity (SV)/ pseudospectral velocity (PSV) calculation. FAS, Fourier amplitude spectrum; Rms, root mean square.

time-series analysis in certain cases, the agreement for most cases of interest in earthquake engineering is excellent. The average relative error at 0.05–10 s is only about 5% for cases with a damping ratio of 50% (Fig. 2e,f). Although the average relative error increases with decreasing damping ratio, it is about 15%, even for cases with a damping ratio of 5% (Fig. 2a,b). In addition, we also observe the well-known phenomena that the SV and PSV ordinates are similar (i.e., SV/PSV is near unity) over the intermediate-period range, the SV ordinate is smaller than the PSV ordinate (i.e., SV/PSV < 1) at short oscillator periods, and larger than it (i.e., SV/PSV > 1) at longer oscillator periods; in addition, it increases with the increase in the oscillator period and damping ratio. These phenomena also validate the proposed approach. The results of SV/PSV using the equation of Sadek *et al.* (2000) are also plotted in Figure 2. Because this equation does not incorporate seismological effects, its results are independent of seismological parameters. The results of the equation derived by Sadek *et al.* (2000) are typically consistent with those obtained by the proposed approach for large moment magnitudes and long site-to-source distances.

Figures 2–4 show that the accuracy of the proposed approach deteriorates for cases with extremely short oscillator periods. When the oscillator period is shorter than about 0.05 s, the relative error increases very quickly and may exceed 30%. This is possibly caused by the assumption that the oscillator-response duration for SV D_{rms} is the same as that for PSV

Dp_{rms} . Therefore, formulating a more accurate equation for the oscillator-response duration for SV D_{rms} may reduce the error of the proposed approach, which will be the focus of our future studies.

THEORETICAL EXPLORATION OF SEISMOLOGICAL EFFECTS

Seismological effects

In this section, the effects of moment magnitude, site-to-source distance, and site conditions on the SV–PSV relationship are explored. It is evident from Figure 2 that the SV–PSV relationship strongly and slightly depends on the moment magnitude at long and short oscillator periods, respectively. The average values of SV/PSV at two periodic bands, 0.03–0.07 and 1–3 s, are used to quantify the influence of the moment magnitude on the SV–PSV relationship at short and long oscillator periods, respectively. For the cases in Figure 2, a 100% increase in the moment magnitude decreases the average value of SV/PSV at 1–3 s by 83%, whereas it decreases that at 0.03–0.07 s by only 21%. It is already known that the SV–PSV relationship depends on the oscillator period and damping ratio. By comparing Figures 2 and 4, the degree of dependency on the

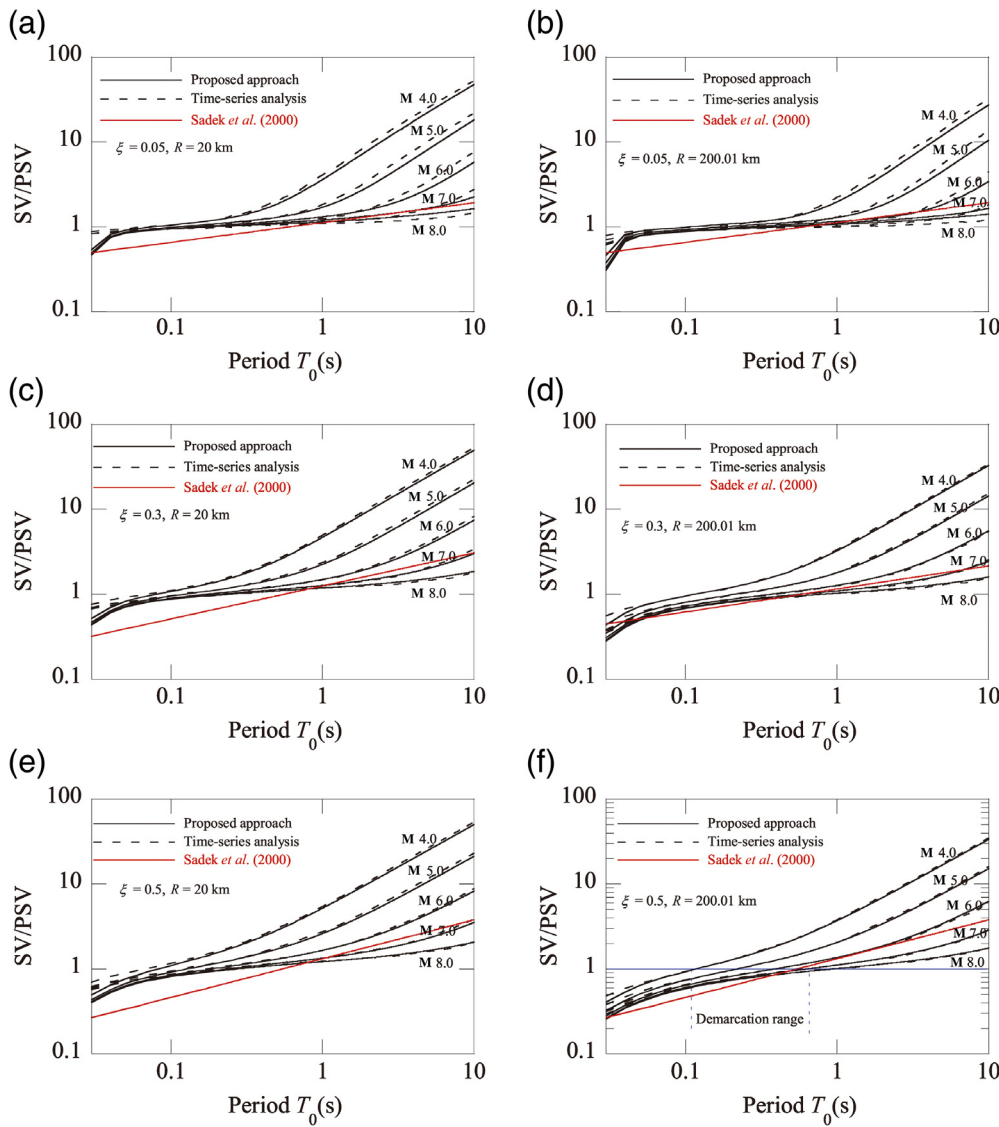


Figure 2. Comparison between SV/PSV results of proposed approach, time-series analysis, and equation of Sadek et al. (2000), considering various moment magnitudes for cases with (a) $\xi = 0.05$ and $R = 20$ km, (b) $\xi = 0.05$ and $R = 200.01$ km, (c) $\xi = 0.3$ and $R = 20$ km, (d) $\xi = 0.3$ and $R = 200.01$ km, (e) $\xi = 0.5$ and $R = 20$ km, and (f) $\xi = 0.5$ and $R = 200.01$ km. The color version of this figure is available only in the electronic edition.

moment magnitude is found to be much more significant than that on the damping ratio. For the cases in Figure 4, a 100% increase in the damping ratio increases the average value of SV/PSV at 1–3 s by only 5.1%, which is considerably smaller than the change rate (83%) caused by the moment magnitude. Figure 2 shows that the SV/PSV ratio approaches unity, that is, the SV approaches PSV, with the increase in the moment magnitude at long oscillator periods. However, this trend is reversed at short oscillator periods. The demarcation range beyond which the opposite trend is observed (Fig. 2f) varies with the site-to-source distance. For the cases with a site-to-source distance of 20 km (Fig. 2a,c,e), the demarcation range

is at approximately 0.07–0.24 s. In cases with a site-to-source distance of 200.01 km (Fig. 2b,d,f), the demarcation range is at approximately 0.12–0.87 s. Figure 3 indicates that the trend of SV/PSV with the variation in the site-to-source distance is typically consistent with that with the variation in the moment magnitude, but the degree of variation is obviously much smaller. For the cases in Figure 3, a 100% increase in the site-to-source distance decreases the average value of SV/PSV at 1–3 s by only 2.4%, which is much smaller than the change rate (83%) caused by the moment magnitude.

To investigate the effect of site conditions on the SV–PSV relationship, four single-layer soil sites are considered. The site parameters, including the fundamental period T_s , impedance ratio of the soil layer with respect to bedrock I_p , and soil damping ratio h , are presented in Figure 5. The seismic motions at the rock sites are then propagated through the soil sites. The results of the SV/PSV ratio at the soil sites are estimated using the proposed approach, and they are then compared with those at the rock sites. Representative comparisons for the cases with $R = 126.20$ km, $M = 5$ and 7, and $\xi = 20\%$ are shown in Figure 5. It is noted that the effect of site conditions on the SV–PSV relationship is less significant but more complicated than that of the moment magnitude. The values of SV/PSV at short oscillator periods tend to decrease after the seismic wave propagates through the soil layer. However, the values of SV/PSV at long oscillator periods may increase or decrease depending on the site parameters. When the impedance ratio and soil damping ratio are small (Fig. 5d), the SV/PSV ratio tends to increase at long oscillator periods after the seismic wave propagates through the soil layer. By contrast, when the impedance ratio and soil damping ratio are large (Fig. 5a), the SV/PSV ratio at long oscillator periods tends to

decrease after the seismic wave propagates through the soil layer. However, the values of SV/PSV at long oscillator periods may increase or decrease depending on the site parameters. When the impedance ratio and soil damping ratio are small (Fig. 5d), the SV/PSV ratio tends to increase at long oscillator periods after the seismic wave propagates through the soil layer. By contrast, when the impedance ratio and soil damping ratio are large (Fig. 5a), the SV/PSV ratio at long oscillator periods tends to

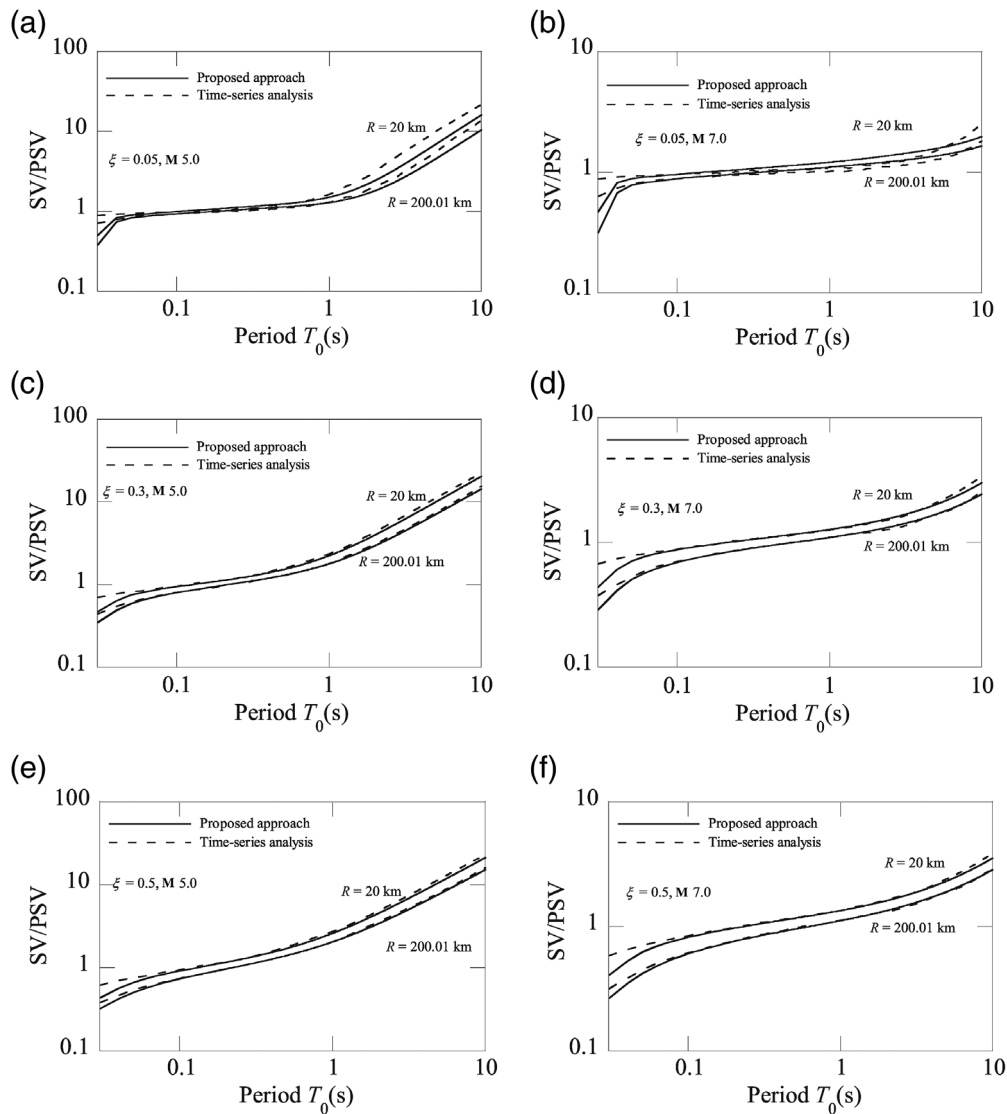


Figure 3. Comparison between SV/PSV results of proposed approach and time-series analysis considering different site-to-source distances for cases with (a) $\xi = 0.05$ and $M = 5.0$, (b) $\xi = 0.05$ and $M = 7.0$, (c) $\xi = 0.3$ and $M = 5.0$, (d) $\xi = 0.3$ and $M = 7.0$, (e) $\xi = 0.5$ and $M = 5.0$, and (f) $\xi = 0.5$ and $M = 7.0$.

decrease. When the fundamental period is long (Fig. 5c), the decrease is more considerable.

Explanation

To explain the previous phenomena in the RVT framework, equation (5) is analyzed. The results for the two terms in equation (5), that is, the rms ratio R_{rms} and peak factor ratio R_{pf} for the cases in Figure 2, are shown in Figures 6 and 7, respectively. It can be seen that the results of the rms ratio are very similar to those of SV/PSV, and the results of the peak factor ratio are near unity. This means that SV/PSV is governed by the rms ratio, which facilitates the explanation of the previous phenomena based on the rms ratio.

Because the oscillator-response durations for the SV and PSV are assumed to be the same, the rms ratio equals the square of the ratio of $\int_0^\infty |Y(\omega)Hv(\omega, \bar{\omega}, \xi)|^2 d\omega$ to $\int_0^\infty |Y(\omega)Hpv(\omega, \bar{\omega}, \xi)|^2 d\omega$. Moreover, $\int_0^\infty |Y(\omega)Hv(\omega, \bar{\omega}, \xi)|^2 d\omega$ and $\int_0^\infty |Y(\omega)Hpv(\omega, \bar{\omega}, \xi)|^2 d\omega$ on the numerator and denominator can be considered the areas of the square of the oscillator-response FAS for the SV and PSV, respectively. When the areas of SV and PSV are similar, SV/PSV is near unity. When the area of SV is larger than that of PSV, SV/PSV is larger than unity. In contrast, when the area of SV is smaller than that of PSV, SV/PSV is smaller than unity. From equation (5), it can be seen that the difference between the two areas, that is, two spectra, is caused by the difference in the oscillator transfer functions. The values of the oscillator transfer functions of SV and PSV are compared in Figure 8. Here, T denotes the period of FAS corresponding to $\omega (T = 2\pi/\omega)$. It can be seen that the values of the two transfer functions are similar around the oscillator period T_0 . However, at periods shorter than the oscillator period T_0 , the values of

$|Hv(\omega, \bar{\omega}, \xi)|$ are larger than those of $|Hpv(\omega, \bar{\omega}, \xi)|$; at periods longer than the oscillator period T_0 , the relationship is opposite. When the damping ratio is increased, the values of the two oscillator transfer functions at periods around the oscillator period T_0 (i.e., the similar part) decrease, but those at other shorter and longer periods almost do not vary.

Based on the properties of $|Hv(\omega, \bar{\omega}, \xi)|$ and $|Hpv(\omega, \bar{\omega}, \xi)|$, the well-known trends of SV/PSV with variations in the oscillator period and damping ratio can be clearly explained. Figure 9 indicates that when the oscillator period is short, the period range that is longer than the oscillator period is wide, in which $|Hpv(\omega, \bar{\omega}, \xi)| > |Hv(\omega, \bar{\omega}, \xi)|$. Thus, the area of PSV $\int_0^\infty |Y(\omega)Hpv(\omega, \bar{\omega}, \xi)|^2 d\omega$ is larger than that of SV $\int_0^\infty |Y(\omega)Hv(\omega, \bar{\omega}, \xi)|^2 d\omega$. Therefore, SV/PSV is smaller than

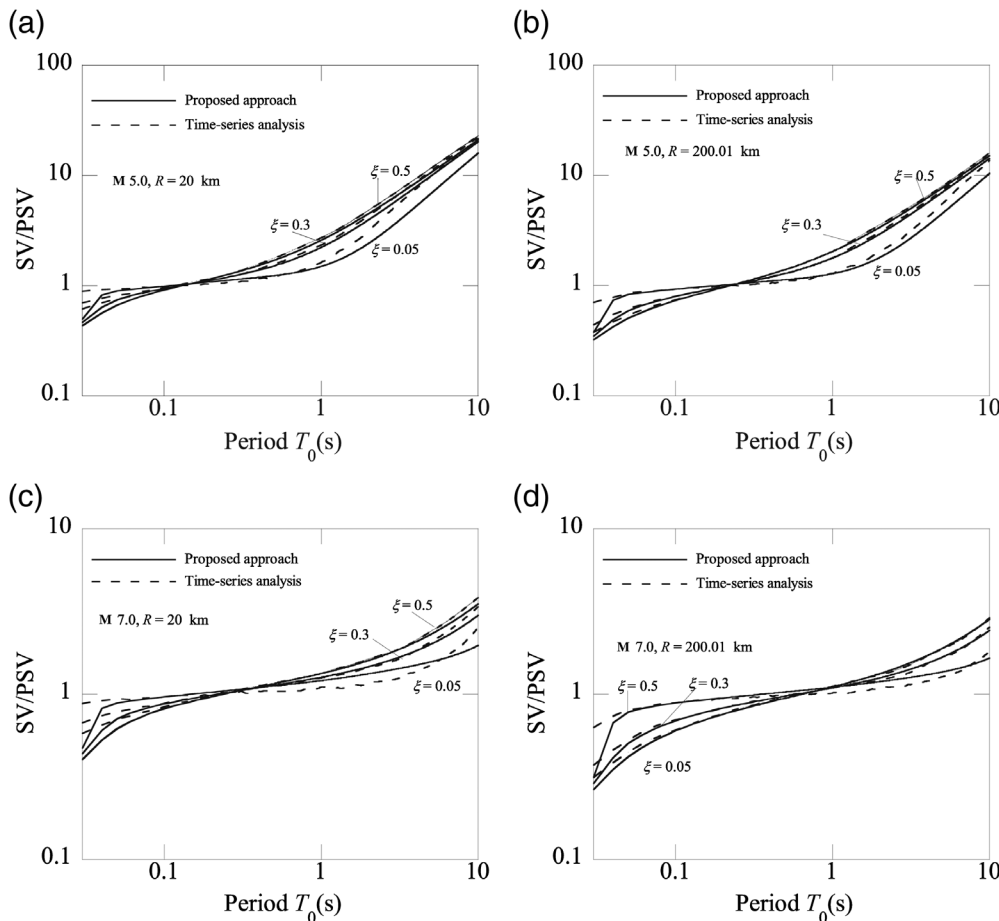


Figure 4. Comparison between SV/PSV results of proposed approach and time-series analysis considering different damping ratios for cases with (a) $M = 5.0$ and $R = 20$ km, (b) $M = 5.0$ and $R = 200.01$ km, (c) $M = 7.0$ and $R = 20$ km, and (d) $M = 7.0$ and $R = 200.01$ km.

unity (i.e., $SV < PSV$) at short oscillator periods, as shown in Figures 2–4. As the oscillator period is increased, the period range that is shorter than the oscillator period increases, in which $|Hv(\omega, \bar{\omega}, \xi)| > |Hpv(\omega, \bar{\omega}, \xi)|$. Thus, the area of SV increases relative to that of PSV. When the oscillator period is increased to some extent, the areas of the two spectra are virtually identical. Therefore, SV/PSV is near unity over the intermediate-period range (i.e., $SV \approx PSV$). As the oscillator period is further increased, the area of SV becomes larger than that of PSV and increases with the oscillator period. Therefore, SV/PSV is larger than unity (i.e., $SV > PSV$) at long oscillator periods and increases with the oscillator period, as shown in Figures 2–4.

As for the trend of SV/PSV with the variation in the damping ratio, because the similar part of the two oscillator transfer functions around the oscillator period decreases with the increasing damping ratio (Fig. 8), the similarity between the areas of SV and PSV decreases, or their difference increases. Therefore, SV/PSV deviates from unity with the increase in the damping ratio, as shown in Figure 4. This also explains why SV/PSV

increases at long oscillator periods and decreases at short oscillator periods with the increase in the damping ratio.

The trends of SV/PSV with the variation in the moment magnitude and site-to-source distance can also be clearly explained based on the rms ratio. It can be seen from equation (5) that the seismological parameters influence the SV–PSV relationship by changing the FAS. Because the FAS affects both the numerator and denominator of the rms ratio, it is its relative values at different periods rather than its absolute values, which really affect SV/PSV. This point can be understood by scaling the FAS by a constant value. Because the constant value will exist on the numerator and denominator of the rms ratio and then disappear, the rms ratio does not change. In addition, the relative values of FAS at different periods represent the frequency content of ground motion. Therefore, the seismological effects on SV/PSV are governed by the ground-motion frequency content.

Figure 10 indicates that, when the moment magnitude and site-to-source distance increase, the long-period components relatively increase. The values of FAS at long periods increase more quickly than those at short periods (Fig. 10a), and the values of FAS at short periods decrease more quickly than those at long periods (Fig. 10b). Because $|Hpv(\omega, \bar{\omega}, \xi)| > |Hv(\omega, \bar{\omega}, \xi)|$ at long periods, the area of PSV increases relative to that of SV with the increase in the moment magnitude and site-to-source distance. Therefore, SV/PSV decreases with the increase in the moment magnitude and site-to-source distance. Because SV/PSV is smaller than unity at short oscillator periods and larger than unity at long oscillator periods, the SV approaches the PSV at long oscillator periods and deviates from the PSV at short oscillator periods with the increase in the moment magnitude and site-to-source distance, as shown in Figures 2 and 3. Because the variation in the frequency content with the moment magnitude is more significant than that with the site-to-source distance (Fig. 10), the variation in SV/PSV with the moment magnitude is more significant.

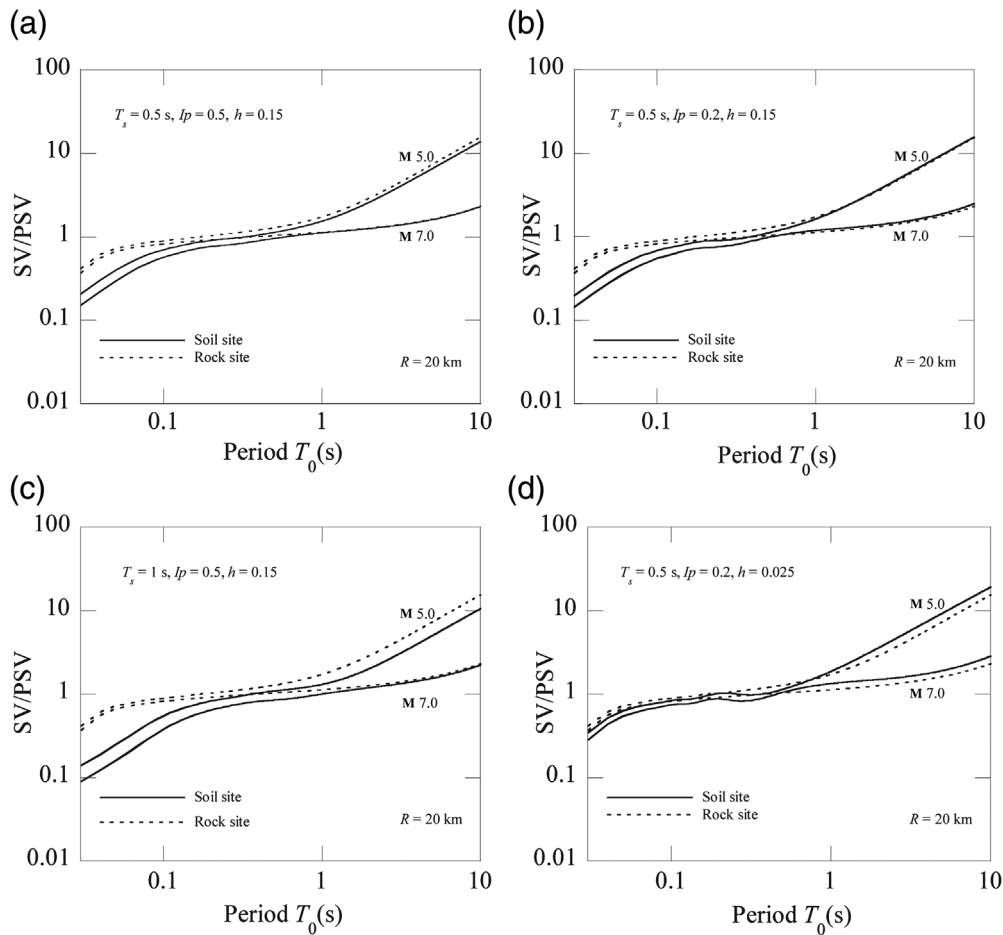


Figure 5. Comparison between SV/PSV results at rock and soil sites with (a) $T_s = 0.5$ s, $l_p = 0.5$, and $h = 0.15$; (b) $T_s = 0.5$ s, $l_p = 0.2$, and $h = 0.15$; (c) $T_s = 1$ s, $l_p = 0.5$, and $h = 0.15$; and (d) $T_s = 0.5$ s, $l_p = 0.2$, and $h = 0.025$.

To explain the trends in SV/PSV with the variation in site parameters observed in Figure 5, the FAS values at the soil and rock sites are compared in Figure 11. The dotted and solid lines represent the FAS values at the rock and soil sites, respectively. The variation in FAS with the site conditions is found to be more complicated than that with the moment magnitude and site-to-source distance. The FAS values at short periods decrease, whereas those at periods around the site fundamental period increase, and those at long periods remain unchanged, after the seismic wave propagates through the soil sites. This is because the soil site acts as a filter and alters the FAS when the seismic wave propagates through the soil site. Moreover, the site amplification ratios are larger than unity at periods around the site fundamental period and decrease toward unity and zero at long and short periods, respectively (Zhang and Zhao, 2017, 2018). Therefore, the components at short periods decrease, and those at periods around the site fundamental period relatively increase after the seismic wave propagates

through the soil site. When the oscillator period is short and less than the site fundamental period, the components with periods longer than the oscillator period increase relative to those with periods shorter than the oscillator period. Because $|Hp\nu(\omega, \bar{\omega}, \xi)| > |H\nu(\omega, \bar{\omega}, \xi)|$ at long periods, the area of PSV increases relative to that of SV. Therefore, at short oscillator periods, SV/PSV decreases after the seismic wave propagates through the soil sites. However, at long oscillator periods (longer than the site fundamental period), the situation is more complex. When the impedance ratio and soil damping ratio are small (Fig. 11d), the site amplification ratios at periods around the site fundamental period are large, and the amplified FAS values are more significant than the decreased values at very short periods. Thus, the values of full components at periods shorter than the oscillator period relatively increase. In addition, $|H\nu(\omega, \bar{\omega}, \xi)|$ is larger than $|Hp\nu(\omega, \bar{\omega}, \xi)|$ at the periods shorter than the oscillator periods, as shown

in Figure 8. Therefore, at long oscillator periods, the area of SV increases relative to that of PSV (or SV/PSV increases) for such cases. By contrast, when the impedance ratio and soil damping ratio are large (Fig. 11a), the site amplification ratios at periods around the fundamental period are small, the decreased FAS values at short periods are more significant than the increased values at periods around the site fundamental period. Thus, the values of full components at periods shorter than the oscillator period relatively decrease. Therefore, at long oscillator periods, the area of SV decreases relative to that of PSV (or SV/PSV decreases) for such cases. When the site fundamental period is long (Fig. 11c), the decrease range of FAS increases, and SV/PSV at long oscillator periods further decreases.

STATISTICAL EXPLORATION OF SEISMOLOGICAL EFFECTS

The seismological effects on the SV–PSV relationship are further explored based on the statistical analyses of real seismic

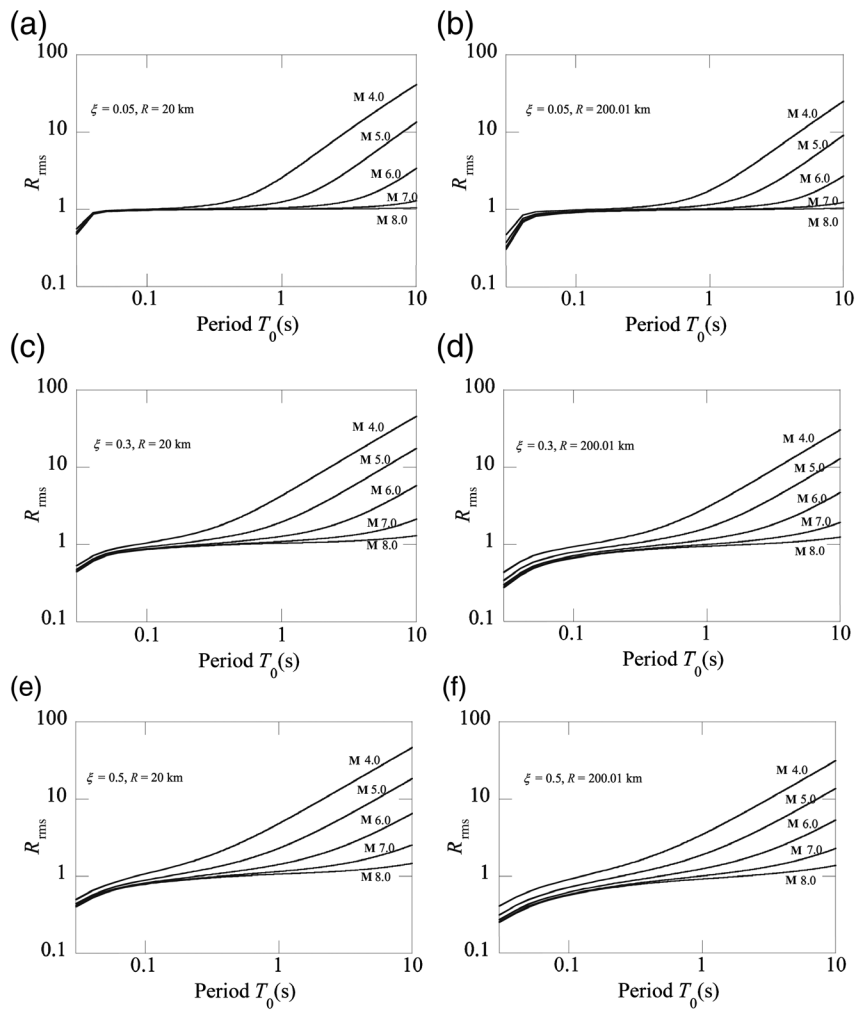


Figure 6. Values of rms ratio R_{rms} for cases with (a) $\xi = 0.05$ and $R = 20$ km, (b) $\xi = 0.05$ and $R = 200.01$ km, (c) $\xi = 0.3$ and $R = 20$ km, (d) $\xi = 0.3$ and $R = 200.01$ km, (e) $\xi = 0.5$ and $R = 20$ km, and (f) $\xi = 0.5$ and $R = 200.01$ km.

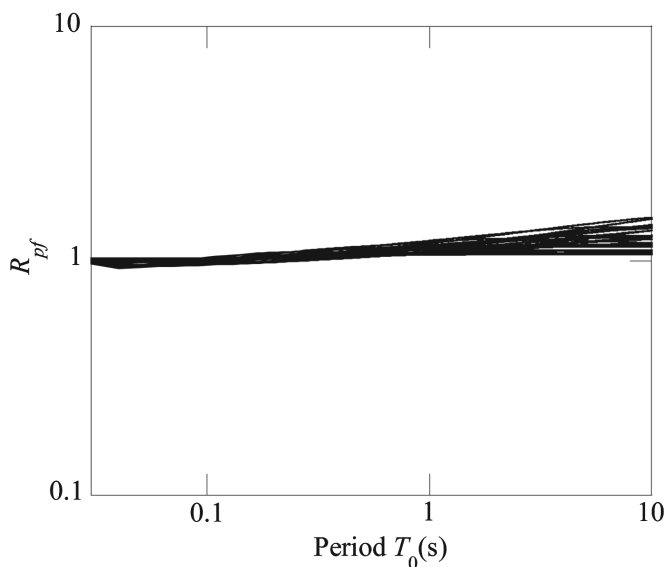


Figure 7. Values of peak-factor ratio R_{pf} for all cases in Figure 2.

records. To this end, a total of 11,700 horizontal acceleration-time histories (5850 seismic ground motions) with a wide variation in magnitude (4.0–9.0) and epicentral distance (10–200 km) are selected from the strong-motion seismograph networks (K-NET and KiK-net) of Japan (National Research Institute for Earth Science and Disaster Resilience [NIED], 1995). The peak ground-motion acceleration of each record is larger than 20 gal to guarantee a sufficient signal-to-noise ratio. These seismic ground motions were recorded at 223 stations that cover the four site classes (classes B, C, D, and E) defined in the National Earthquake Hazards Reduction Program (NEHRP) (2000). For many K-NET stations, the PS logging is down to a depth of 20 m. For these sites, the average shear-wave velocity in the upper 30 m, V_{S30} , used for site classification is converged from that in the upper 20 m, V_{S20} , based on the correlation equation of Kanno *et al.* (2006) ($V_{S30} = 1.13V_{S20} + 19.5$). The distributions of magnitude M_j and

epicentral distance d for the four site classes are shown in Figure 12. The magnitude M_j adopted in the K-NET and KiK-net is the Japan Meteorological Agency (JMA) magnitude. Different from the moment magnitude determined based on the seismic moment, the magnitude defined by the JMA is determined based on the maximum displacements and velocities calculated from recorded accelerations (see Data and Resources). To investigate the effects of magnitude, epicentral distance, and site conditions on the SV–PSV relationship, the selected seismic records are classified into 36 groups, as summarized in Table 1. Because of the lack of sites belonging to class A (three sites), only two ground motions that satisfied the previous conditions were recorded on such sites by investigating all of the K-NET and KiK-net stations. Because of the lack of statistical significance, the two ground motions are excluded in the statistical analysis.

The value of SV/PSV for each record is calculated using the direct integration method of Nigam and Jennings (1969).

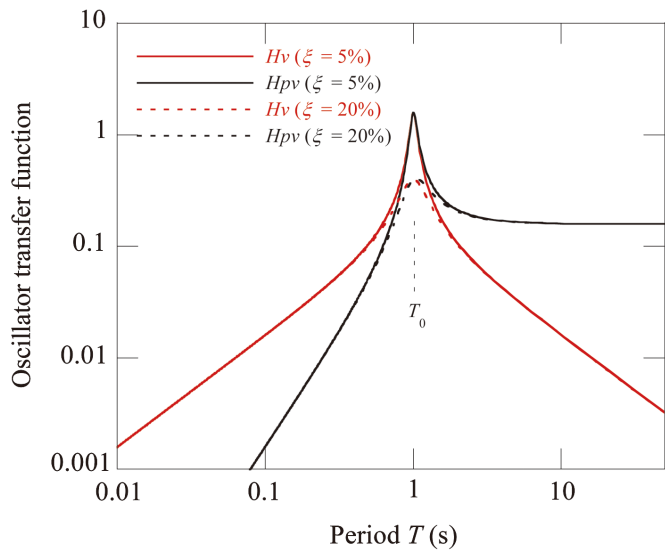


Figure 8. Comparison of oscillator transfer functions for SV and PSV. The color version of this figure is available only in the electronic edition.

The oscillator periods and damping ratios considered for the calculation are similar to those used in Figures 2–4. The results of SV/PSV for each group are then averaged, and parts of them are used as representatives, as shown in Figures 13–15. It is found that the trend of SV/PSV with the variation in magnitude is consistent with that based on the RVT analysis by the comparison of Figures 2 and 13. SV/PSV approaches unity, that is, SV approaches PSV, with the increase in the moment magnitude at long oscillator periods, but the trend is reversed at short oscillator periods. The demarcation range beyond which the opposite trend is observed varies with the site class and slightly changes with the epicentral distance. For the cases in classes B–E, the demarcation ranges are located at approximately 0.1–0.15, 0.15–0.25, 0.2–0.4, and 0.3–0.7 s, respectively. Figure 13 also supports that SV/PSV increases with the damping ratio at long oscillator periods but decreases at short oscillator periods. Figure 14 indicates that, similar to the results based on the RVT analyses, the variation degree of SV/PSV with the epicentral distance is much smaller than that with the magnitude. However, a clear trend of SV/PSV with the variation in the epicentral distance cannot be

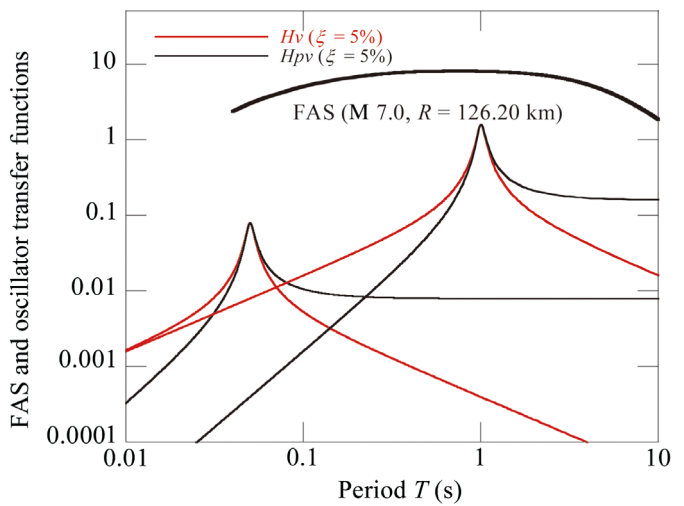


Figure 9. Variation in oscillator transfer functions for SV and PSV with oscillator period. The color version of this figure is available only in the electronic edition.

observed from the statistical analyses in Figure 14. Although only the results of site classes C and D are shown in Figures 13 and 14, the same trends of SV/PSV with variations in magnitude and epicentral distance can also be observed from the results of site classes B and E. In addition, similar to the results based on the RVT analyses, Figure 15 indicates that the effect of site conditions is less significant but more complicated than that of magnitude. The values of SV/PSV at short oscillator periods gradually decrease from hard rock to soft soil, but the values at long oscillator periods may increase or decrease.

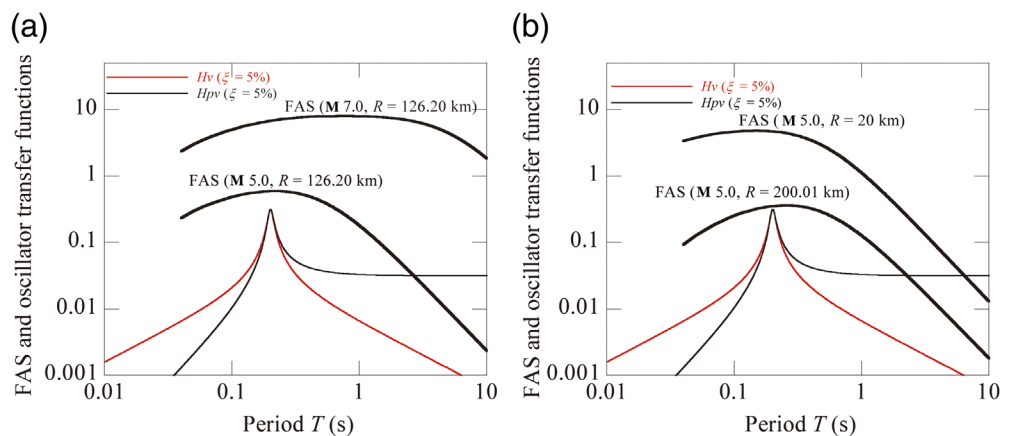


Figure 10. Effects of (a) moment magnitude and (b) site-to-source distance on FAS. The color version of this figure is available only in the electronic edition.

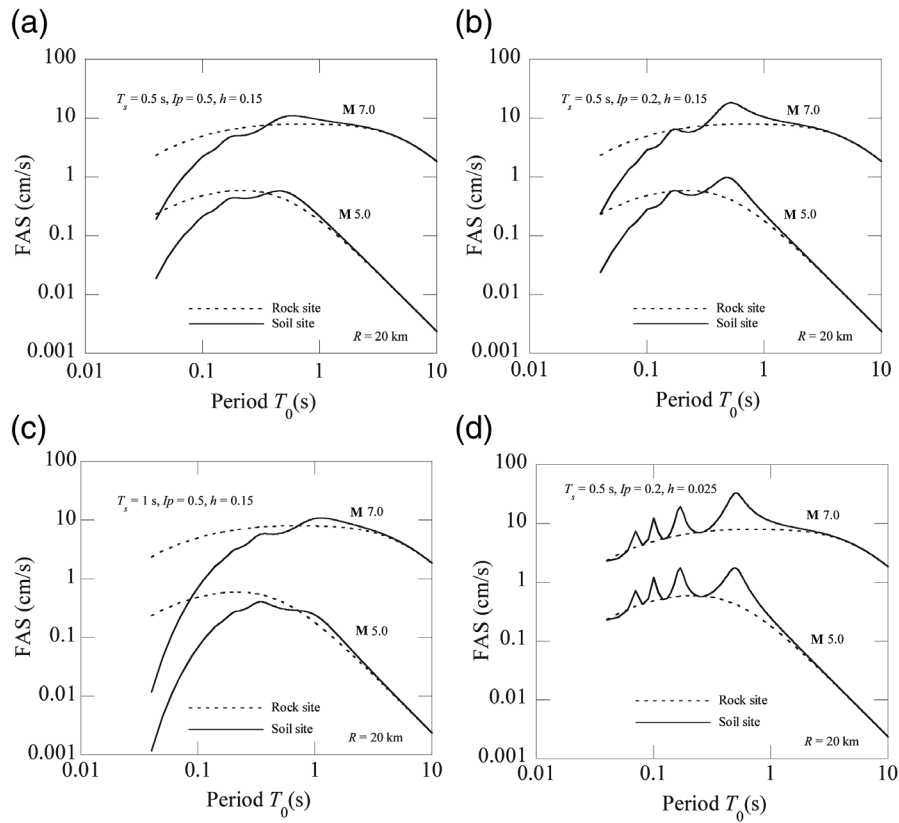


Figure 11. Effects of site conditions on FAS for cases with (a) $T_s = 0.5$ s, $l_p = 0.5$, and $h = 0.15$; (b) $T_s = 0.5$ s, $l_p = 0.2$, and $h = 0.15$; (c) $T_s = 1$ s, $l_p = 0.5$, and $h = 0.15$; and (d) $T_s = 0.5$ s, $l_p = 0.2$, and $h = 0.025$.

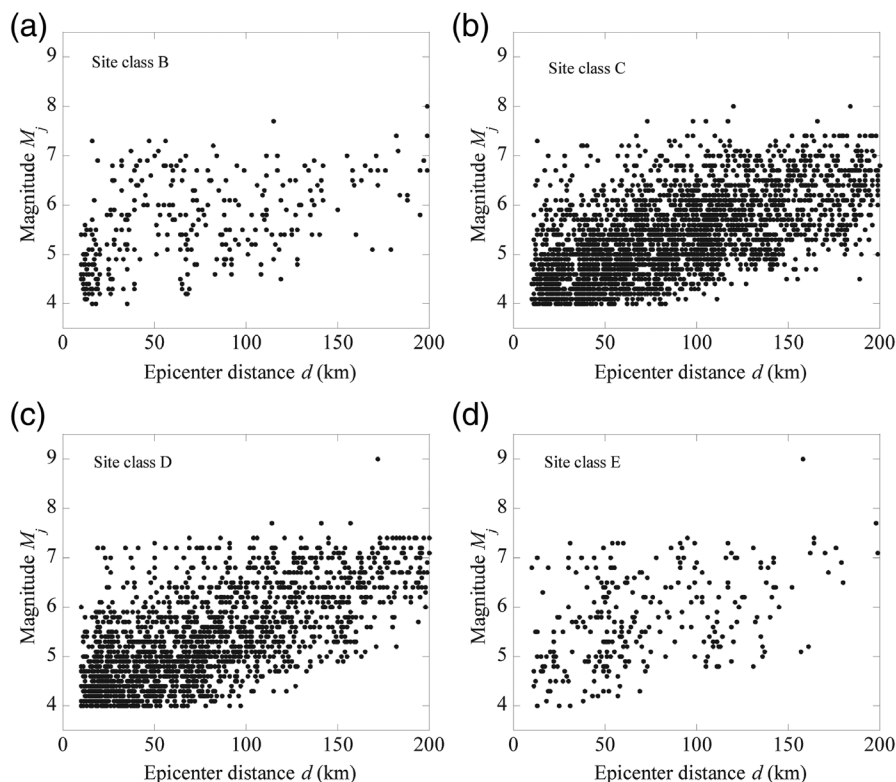


Figure 12. Magnitude M_j versus epicentral distance d for site classes (a) B, (b) C, (c) D, and (d) E.

CONCLUSIONS

To investigate the seismological effects on the SV–PSV relationship, in this study, an approach for estimating the ratio of SV to PSV based on the RVT is proposed, and it is verified by comparing its results with those of traditional time-series analyses. For most cases of interest in earthquake engineering, the accuracy of the proposed approach is high but deteriorates when the oscillator period is very short (<0.05 s). This is possibly because of the assumption that the oscillator-response durations for SV and PSV are the same. A more accurate equation of the oscillator-response duration for the SV may aid in reducing the error of the proposed approach.

Based on the proposed approach, the effects of earthquake magnitude and distance as well as site conditions on the SV–PSV relationship are systematically explored. The observed phenomena are then explained based on the proposed approach by investigating the variation in the ground-motion frequency content. Furthermore, the seismological effects are investigated based on the statistical analyses of real seismic records. The findings can be summarized as follows.

1. The influence of earthquake magnitude compared with those of the distance and site conditions on SV/PSV is more significant. The effects of distance and site conditions on SV/PSV are not that significant and are similar in degree to that of the oscillator damping ratio.

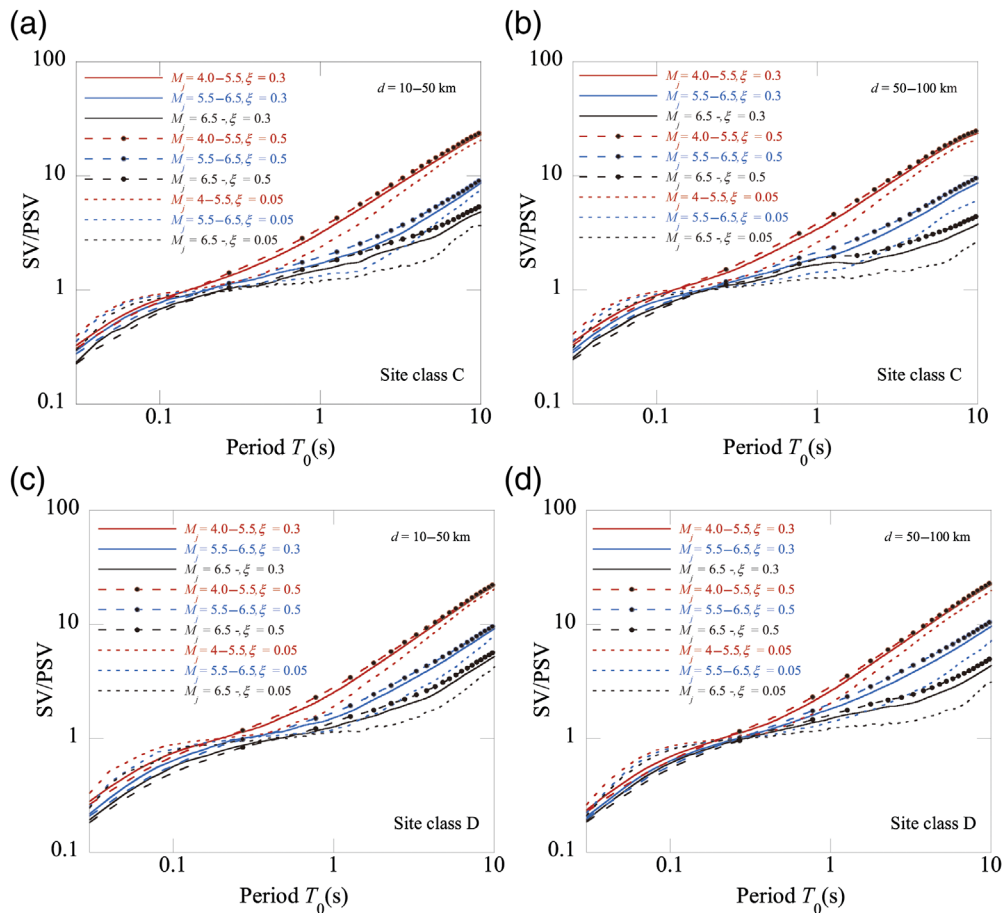


Figure 13. Comparison between results of SV/PSV with different magnitudes and damping ratios for (a) site class C, $d = 10\text{--}50$ km; (b) site class C, $d = 50\text{--}100$ km; (c) site class D, $d = 10\text{--}50$ km; and (d) site class D, $d = 50\text{--}100$ km. The color version of this figure is available only in the electronic edition.

2. The SV/PSV ratio strongly depends on the magnitude at long oscillator periods but slightly depends on it at short oscillator periods. A 100% increase in the moment magnitude decreases the average value of SV/PSV at periods of 1–3 s by 83%, whereas it decreases that at periods of 0.03–0.07 s by only 21%. The SV approaches PSV with increasing magnitudes at long oscillator periods but performs oppositely at short oscillator periods. The demarcation range beyond which the opposite trend is observed varies from (0.07–0.24) to (0.12–0.87) s using the proposed approach and considering the regions of central and eastern North America. It varies from (0.1–0.15) to (0.3–0.7) s based on the results obtained by the statistical analysis of seismic records in Japan.

TABLE 1
Classification of Accelerograms Based on Site Class, Magnitude, and Epicentral Distance

Site Class	Magnitude (M_j)	Epicentral Distance (d)	Record Count	Group Number	Site Class	Magnitude (M_j)	Epicentral Distance (d)	Record Count	Group Number		
B	$4.0 \leq M_j < 5.5$	$10 \leq d < 50$	52	1	D	$4.0 \leq M_j < 5.5$	$10 \leq d < 50$	803	19		
		$50 \leq d < 100$	44	2			$50 \leq d < 100$	783	20		
		$100 \leq d \leq 200$	22	3			$100 \leq d \leq 200$	353	21		
	$5.5 \leq M_j < 6.5$	$10 \leq d < 50$	28	4		$5.5 \leq M_j < 6.5$	$10 \leq d < 50$	97	22		
		$50 \leq d < 100$	49	5			$50 \leq d < 100$	284	23		
		$100 \leq d \leq 200$	27	6			$100 \leq d \leq 200$	523	24		
	$M_j \geq 6.5$	$10 \leq d < 50$	16	7		$M_j \geq 6.5$	$10 \leq d < 50$	16	25		
		$50 \leq d < 100$	32	8			$50 \leq d < 100$	53	26		
		$100 \leq d \leq 200$	28	9			$100 \leq d \leq 200$	256	27		
C	$4.0 \leq M_j < 5.5$	$10 \leq d < 50$	663	10	E	$4.0 \leq M_j < 5.5$	$10 \leq d < 50$	91	28		
		$50 \leq d < 100$	489	11			$50 \leq d < 100$	44	29		
		$100 \leq d \leq 200$	136	12			$100 \leq d \leq 200$	22	30		
		$5.5 \leq M_j < 6.5$	$10 \leq d < 50$	82			13	$5.5 \leq M_j < 6.5$	$10 \leq d < 50$	27	31
			$50 \leq d < 100$	192			14		$50 \leq d < 100$	34	32
			$100 \leq d \leq 200$	235			15		$100 \leq d \leq 200$	32	33
	$M_j \geq 6.5$	$10 \leq d < 50$	14	16		$M_j \geq 6.5$	$10 \leq d < 50$	17	34		
		$50 \leq d < 100$	48	17			$50 \leq d < 100$	22	35		
		$100 \leq d \leq 200$	206	18			$100 \leq d \leq 200$	30	36		

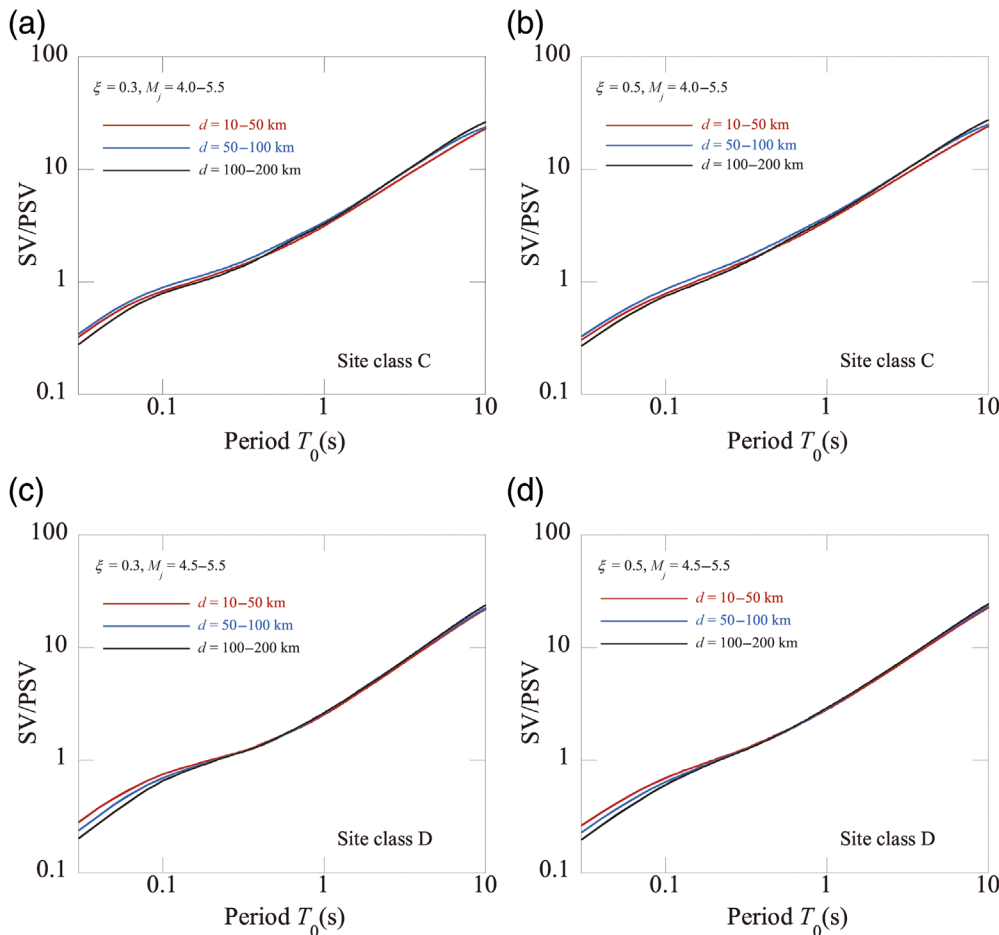


Figure 14. Comparison between results of SV/PSV with different epicentral distances for (a) site class C, $\xi = 0.3$, and $M_j = 4.0-5.5$; (b) site class C, $\xi = 0.5$, and $M_j = 4.0-5.5$; (c) site class D, $\xi = 0.3$, and $M_j = 4.0-5.5$; and (d) site class D, $\xi = 0.5$, and $M_j = 4.0-5.5$. The color version of this figure is available only in the electronic edition.

3. For the results of the proposed approach considering the regions of central and eastern North America, the trend of SV/PSV with the variation in distance is consistent with that of the variation in magnitude. However, based on the results of the statistical analysis using seismic records in Japan, the trend of SV/PSV with the variation in distance is not obvious.
4. The effect of site conditions on SV/PSV is more complicated than that of magnitude and distance. The values of SV/PSV at short oscillator periods gradually decrease from hard-rock to soft-soil sites; however, those at long oscillator periods may increase or decrease depending on specific site parameters.
5. The seismological effects on SV/PSV are governed by the ground-motion frequency content. Therefore, in practical seismic design, a parameter reflecting the ground-motion frequency content should be incorporated in the formulation that relates SV to PSV.

6. Only the regions of central and eastern North America were considered in the discussions using the proposed approach. For other world regions, the values of SV/PSV may differ because SV and PSV can vary; nevertheless, the trends of SV/PSV with magnitude, distance, and site conditions are basically consistent. This can be ascertained by comparing the results of the proposed method and statistical analysis of seismic records in Japan.

DATA AND RESOURCES

The stochastic time series used in the analysis were created using the Stochastic-Method SIMulation (SMSIM) programs obtained from http://daveboore.com/software_online.html (last accessed April 2020). Random vibration theory analyses were performed using scripts written in MATLAB (<http://www.mathworks.com>, last accessed April 2020). All strong-motion records used in this study can be downloaded from <http://www.kyoshin.bosai.go.jp/> (last accessed November 2020). The magnitude defined by the Japan

Meteorological Agency (JMA) is determined based on the maximum displacements and velocities calculated from recorded accelerations (https://www.data.jma.go.jp/svd/eqev/data/bulletin/catalog/notes_e.html, last accessed April 2021).

DECLARATION OF COMPETING INTERESTS

The authors acknowledge that there are no conflicts of interest recorded.

ACKNOWLEDGMENTS

This study was partially supported by the National Natural Science Foundation of China (Grant Number 51738001), and the support is gratefully acknowledged. The authors are also grateful to Zheng Liu for assisting in the preparation of figure illustrations in this article and Baojian Hang and Jia Deng for aiding in the selection of earthquake data. The authors thank Editor-in-Chief Thomas Pratt and two anonymous reviewers for their perceptive and useful comments, which led to significant improvements in the article.

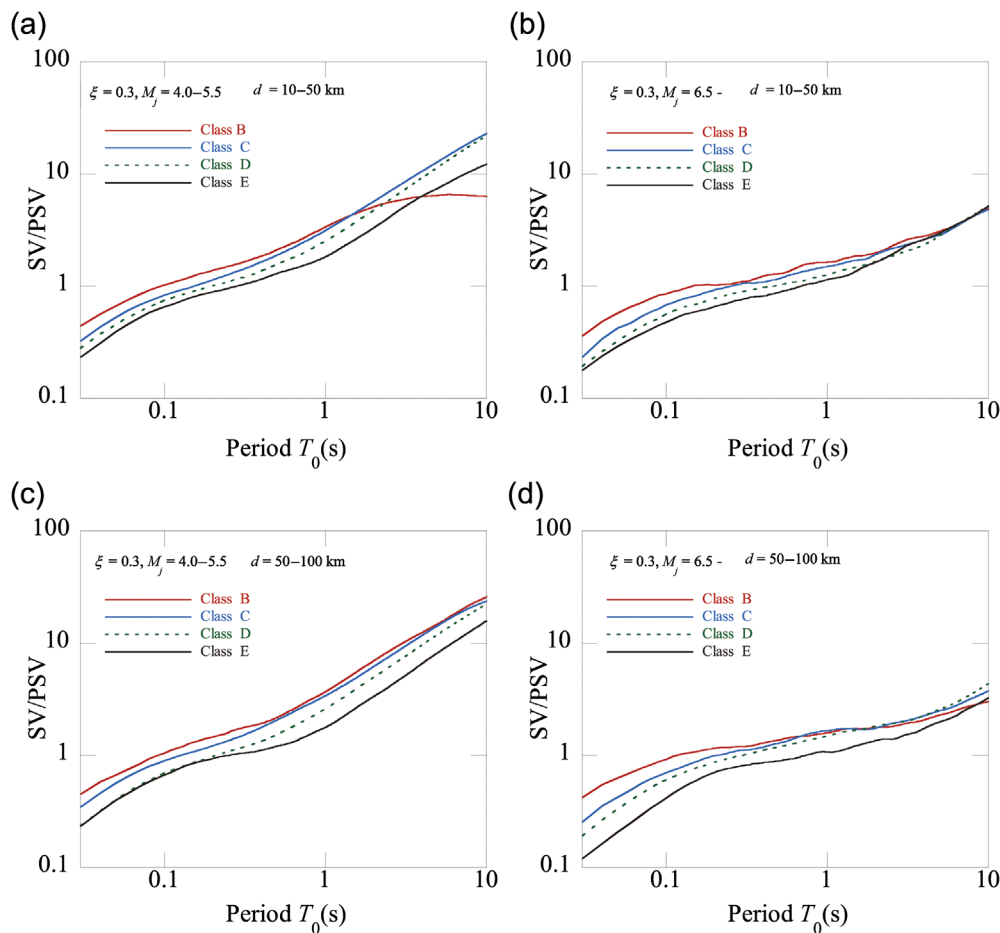


Figure 15. Comparison between results of SV/PSV in different site classes for cases with (a) $\xi = 0.3$, $M_j = 4-5.5$, and $d = 10-50$ km; (b) $\xi = 0.3$, $M_j = 6.5-$, and $d = 10-50$ km; (c) $\xi = 0.3$, $M_j = 4-5.5$, and $d = 50-100$ km; and (d) $\xi = 0.3$, $M_j = 6.5-$, and $d = 50-100$ km. The color version of this figure is available only in the electronic edition.

REFERENCES

- ASCE/SEI7-10 (2011). *Minimum Design Loads for Buildings and Other Structures*, Structural Engineering Institute (SEI), American Society of Civil Engineers (ASCE), U.S.A.
- Boore, D. M. (1983). Stochastic simulation of high-frequency ground motions based on seismological models of the radiated spectra, *Bull. Seismol. Soc. Am.* **736**, 1865-1894.
- Boore, D. M. (2003). Simulation of ground motion using the stochastic method, *Pure Appl. Geophys.* **60**, 635-676.
- Boore, D. M. (2005). SMSIM—Fortran programs for simulating ground motions from earthquakes: Version 2.3, *U.S. Geol. Surv. Open-File Rept. OFR 96-80-A*, Menlo Park, California.
- Boore, D. M., and E. M. Thompson (2015). Revisions to some parameters used in stochastic-method simulations of ground motion, *Bull. Seismol. Soc. Am.* **105**, 1029-1041.
- Cartwright, D. E., and M. S. Longuet-Higgins (1956). The statistical distribution of the maxima of a random function, *Proc. Math. Phys. Sci.* **237**, 212-223.
- Davenport, A. G. (1964). Note on the distribution of the largest value of a random function with application to gust loading, *Proc. Inst. Civ. Eng.* **28**, 187-196.
- Desai, R. S., and S. N. Tande (2017). Estimation of spectral velocity at long periods for application in velocity dependent seismic energy management devices, *J. Struct. Eng.* **44**, no. 1, 14-22.
- Desai, R. S., and S. N. Tande (2018). Estimate of peak relative velocity from conventional spectral velocity for response spectrum based force evaluation in damping devices, *Structures* **15**, 378-387.
- Eurocode 8 (2004). Design of structures for earthquake resistance, part 1: General rules, seismic actions and rules for buildings, EN 2004-1-1, European Committee for Standardization (CEN), Brussels, Belgium.
- Federal Emergency Dissipation Agency (FEMA-450) (2003). *NEHRP recommended provisions for seismic regulations for new buildings and other structures. Part 1: Provisions and Part 2: Commentary*, FEMA P-2082-1, Washington, D.C.
- Gupta, V. K. (2009). A new approximation for spectral velocity ordinates at short periods, *Earthq. Eng. Struct. Dynam.* **38**, 941-949.
- Kanno, T., A. Narita, N. Morikawa, H. Fujiwara, and Y. Fukushima (2006). A new attenuation relation for strong ground motion in Japan based on recorded data, *Bull. Seismol. Soc. Am.* **96**, no. 3, 879-897.
- National Earthquake Hazards Reduction Program (NEHRP) (2000). *Recommended provisions for seismic regulations for new buildings and other structures*, Federal Emergency Management Agency, Washington, D.C.
- National Research Institute for Earth Science and Disaster Resilience (NIED) (1995). Strong motion seismograph networks (K-NET, KIK-net), available at <http://www.kyoshin.bosai.go.jp/kyoshin/> (last accessed December 2020).
- Nigam, N., and P. Jennings (1969). Calculation of response spectra from strong-motion earthquake records, *Bull. Seismol. Soc. Am.* **59**, no. 2, 909-922.
- Pal, A., and V. K. Gupta (2021). A note on spectral velocity approximation at shorter intermediate periods, *Soil Dynam. Earthq. Eng.* **141**, 106422, doi: [10.1016/j.soildyn.2020.106422](https://doi.org/10.1016/j.soildyn.2020.106422).
- Papagiannopoulos, G. A., G. D. Hatzigeorgiou, and B. E. Dimitri (2013). Recovery of spectral absolute acceleration and spectral relative velocity from their pseudo-spectral counterparts, *Earthq. Struct.* **4**, no. 5 489-508.

- Rathje, E. M., and M. C. Ozbey (2006). Site-specific validation of random vibration theory-based seismic site response analysis, *J. Geotech. Geoenviron. Eng.* **132**, no. 7, 911–922.
- Sadek, F., B. Mohraj, and M. A. Riley (2000). Linear static and dynamic procedures for structures with velocity-dependent dampers, *J. Struct. Eng.* **128**, no. 8, 887–895.
- Samdaria, N., and V. K. Gupta (2018). A new model for spectral velocity ordinates at long periods, *Earthq. Eng. Struct. Dynam.* **47**, 169–194.
- Song, J., Y. L. Chu, Z. Liang, and G. C. Lee (2007). Estimation of peak relative velocity and peak absolute acceleration of linear SDOF systems, *Earthq. Eng. Eng. Vib.* **6**, no. 1, 1–10.
- Vanmarcke, E. H. (1975). On the distribution of the first-passage time for normal stationary random processes, *J. Appl. Mech.* **42**, 215–220.
- Wang, X., and E. M. Rathje (2016). Influence of peak factors on site amplification from random vibration theory based site-response analysis, *Bull. Seismol. Soc. Am.* **106**, 1–14.
- Zhang, H. Z., and Y. G. Zhao (2017). Simple calculation method of seismic motion amplification ratio corresponding to fundamental period, *J. Struct. Constr. Eng., AIJ* **82**, no. 734, 597–604 (in Japanese).
- Zhang, H. Z., and Y. G. Zhao (2018). A simple approach for estimating the first resonance peak of layered soil profiles, *J. Earthq. Tsunami* **12**, 185,005, doi: [10.1142/S1793431118500057](https://doi.org/10.1142/S1793431118500057).
- Zhang, H. Z., and Y. G. Zhao (2020). Damping modification factor based on random vibration theory using a source-based ground-motion model, *Soil Dynam. Earthq. Eng.* **136**, 106,225, doi: [10.1016/j.soildyn.2020.106225](https://doi.org/10.1016/j.soildyn.2020.106225).

Manuscript received 29 January 2021

Published online 13 July 2021